Analysis of meteorological data and the surface energy balance of McCall Glacier, Alaska

E.J. Klok[1], M. Nolan[1] and M.R. van den Broeke[2]

[1] Water and Environmental Research Institute, Institute of Northern Engineering, 455 Duckering Bldg, University of Alaska Fairbanks, AK, USA

[2] Institute for Marine and Atmospheric Research, Utrecht University, Princetonplein 5, 3584 CC, Utrecht, the Netherlands

Submitted to Journal of Glaciology, 31 January 2005

Contact address:

Lisette Klok

KNMI

Postbus 201

3730 AE De Bilt

The Netherlands

Lisette.Klok@uibk.ac.at

Abstract

We analyzed meteorological data of the period 27 May to 20 August, 2004 from two automatic weather stations on McCall Glacier, Alaska, to study the relationship between climate and ablation. One of the weather stations is located on a mountain ridge and another in the ablation area where we analyzed the energy balance and the specific mass balance. Over this time period, McCall Glacier's ablation area was characterized by an average temperature of 5.3 °C and an average wind speed of 3.1 m s^{-1}, measured at 2.06 and 3.05 m above the surface, respectively. A sonic height ranger and two ablation stakes indicate a specific mass balance of –1.94 ± 0.09 m water equivalent (w.e.) between 15 June to 20 August at the glacier tongue. The specific mass balance calculated from the surface energy balance, –2.06 ± 0.18 m w.e, is in close correspondence to this. The latter is the sum of 0.12 m w.e of snowfall, 0.003 m w.e. of sublimation (i.e. deposition), and –2.18 m w.e. of melt. About 74% of the melt energy is supplied by net radiation. The ice albedo is measured at 0.19, lower than measured in previous years, possibly due to the influence of ash deposits from forest fires.

1. Introduction

As part of the U.S. National Science Foundation's Freshwater Initiative, this paper describes meteorological measurements and the surface energy balance of McCall Glacier. This project aims to document changes in the freshwater inputs in the Arctic hydrological system and how they relate to climate change. Glaciers can provide useful information about historical changes in climate by means of their length or volume changes or ice core analysis. McCall Glacier has the longest history of research in Arctic Alaska and was for this reason selected for continued long-term research into the glaciological component of the freshwater cycle.

The first glacio-meteorological investigations on McCall Glacier took place between 1957 and 1958 as part of the International Geophysical Year (Orvig, 1961). From 1969 to 1971, new glacio-meteorological experiments were carried out by Wendler and Weller (1974) and Wendler and Ishikawa (1974) as part of the International Hydrological Decade. Measurements of air temperature, ice temperature, and ablation, including some temperature-precipitation mass-balance modeling were also conducted during the 1990s (Rabus and Echelmeyer, 1998; Rabus and Echelmeyer, 2002). Recently, as part of the Freshwater Initiative project, Nolan and others (2005) investigated the volume changes of McCall Glacier and Pattyn and others (2005) examined the basal motion of McCall Glacier.

This paper presents new data on the climate and the surface energy balance of McCall Glacier. This information is needed to explain glacier retreat and its sensitivity to changing climate as well as to support future work on spatially-distributed mass-balance modeling and ice-core proxy interpretation. In 2003, several automatic weather stations (AWS) were installed on the ice and in the vicinity of the glacier. In this paper, we mainly describe measurements from two AWS: one located in the ablation area and another on a mountain ridge several hundred meters above the glacier. Information on these stations is given in section 3. We first give a brief description of McCall Glacier, and its climate in section 2. Section 4 contains an analysis of the meteorological measurements for a summer period in 2004. In section 5, we present the energy balance of the glacier surface and discuss its components, as well as the components of the specific mass balance. Section 6 and 7 contain a discussion on the results and the conclusions, respectively.

2. McCall Glacier

McCall Glacier is located at 69°18’N 143°48’ W, in the Romanzof Mountains of the eastern Brooks Range in northeast Alaska (Fig. 1). Like probably all glaciers in the eastern Brooks Range, McCall Glacier has been losing mass over the last century and probably doing so at a rate that is increasing with time since 1890 (Nolan and others, 2005). Since 1890, McCall Glacier retreated about 800 m. Its current length is 7.5 km and its area about 6.5 km^2. The glacier elevation ranges from about 1400 to 2400 m a.s.l., and the equilibrium line altitude ranges from 2000 to 2400 m a.s.l.

The climate of McCall Glacier differs from the arctic climate of the coastal North Slope of the Brooks Range and also from the continental climate of interior Alaska. It is better described by a mountain climate with relatively high precipitation amounts compared to coastal and interior Alaska (Wendler and others, 1974). McCall Glacier receives about 500 mm precipitation per year of which half is snow (Wendler and others, 1974). The precipitation sources are the Bering Sea, about 700 km to the west, and the Arctic Ocean, about 100 km to the north. Wind directions are frequently from the southwest and mean monthly air temperature at 2275 m a.s.l. can range from –30 °C in winter to 0 °C in summer (Wendler and others, 1974).

Compared to mid-latitude glaciers or maritime glaciers, McCall Glacier has a short ablation season (about 2.5 months, often less), a small ablation rate (about 1.5 m ice per year at the glacier tongue), and a small mass-balance gradient (about 0.12 m w.e. per 100 meter altitude). The glacier is therefore characterized by a small mass turnover (Wendler and others, 1972; Wendler and Ishikawa, 1974; Rabus and Echelmeyer, 1998).

McCall Glacier is a polythermal glacier, which is common for glaciers in the Arctic. Internal accumulation and superimposed ice formation occur in the accumulation zone of McCall Glacier (Wakahama and others, 1976; Trabant and Mayo, 1985). Due to this refreezing of melt water, the ice temperature of the accumulation area (–1°C) is higher than the annual mean surface temperature there (–11°C). For McCall Glacier's accumulation area, internal accumulation can be as much as 64% of the annual accumulation (Trabant and Mayo, 1985). One region of the mid-ablation area is strongly suspected to be temperate at the bed and with either sliding or warm-ice deformation accounting for as much as half of the surface motion (Pattyn and others, 2004; Nolan and others, 2005).

3. Weather stations

For our analyses, we used data of two AWS, which were installed in 2003 by the Water and Environmental Research Institute, University of Alaska, Fairbanks. The

AWS located on the glacier is called JJMC (Fig. 1). It is situated in the ablation area at 1715 m a.s.l., about 30 m west and 30 m lower (due to ice melt) from where Wendler and Weller (1974) and Wendler and Ishikawa (1974) carried out their meteorological measurements.

The AWS at JJMC is a floating station such that the sensor heights remain constant throughout the ablation season. Air temperature and relative humidity (HMP45AC Vaisala, with a Young radiation shield) are measured every minute at 1.09, 2.06 and 3.02 m above the surface; these measurements are unventilated. At the same heights, air temperature is also measured with a finewire thermocouple (Campbell FW3). A sonic height ranger (Cambell SR50) continually measures surface elevation changes caused by ablation and snowfall, and several tens of meters away two ablation stakes are used for spatial comparison and redundancy in case of instrument failure. Wind speed and direction (Met One 034B) are measured every five seconds at 1.70 and 3.05 m. A Kipp & Zonen CNR1 measures the four radiation components (incoming and reflected solar radiation, and incoming and outgoing longwave radiation) at 1.44 m above the surface. This sensor is installed parallel to the surface, within 4 degrees accuracy. Finally, a thermistor string measures ice temperatures every 0.5 m until a depth of 13.5 m at JJMC. A CR10x datalogger stores 15-minute averages of all of the above variables.

By comparing the finewire thermocouple and the Vaisala sensor at 2.06 m for the period 27 May to 20 August 2004, we concluded that the Vaisala measurement exceeds the thermocouple temperature on average by 0.16 K. The standard deviation is 0.58 K. Since the thermocouple can be regarded as free of radiation errors, the difference between the two sensors is explained by a radiation error of the Vaisala sensor in the Young radiation shield. This error increases when wind speeds are low and solar radiation is high, as expected in this situation: mean difference and standard deviation between the Vaisala and thermocouple are 1.30 and 1.59 °C, respectively, for situations with wind speeds < 2.0 m s^{-1} and incoming solar radiation > 500 W m^{-2}. In the subsequent analyses, we therefore used the 2.06-m finewire thermocouple temperature instead of the Vaisala, unless stated otherwise.

AHAB (Fig. 1) is the AWS that is located on the mountain ridge above the glacier at 2415 m a.s.l. Here, air temperature and humidity (HMP45AC Vaisala) at 1.0 and 3.0 m, wind speed and direction (Met One 034B) at 3.0 m, and air pressure (Vaisala CS105) are measured. Hourly averages of these variables are stored.

In section 4.2, we will also describe temperature measurements of Stations 1 and 5 on McCall Glacier (Fig. 1). Station 1 is located in the accumulation area at about 2345 m a.s.l. and Station 5 near the glacier snout (1509 m a.s.l.). At these locations, temperature (15-minute averages) is measured at about 0.9 and 2 m above the surface, respectively, with an Onset Computer Corporation 12-bit Temperature Smart Sensor and an Onset H21 Micrologger.

The accuracy of the sensors installed at the various stations is given in Table 1. Between 27 May and 20 August 2004 (Julian day number (JD) 148-233), all stations measured continuously. Therefore average weather conditions, the energy balance and total ablation for this period will be described in this paper.

4. Analysis of meteorological measurements

4.1 Average weather conditions

Weather conditions at McCall Glacier measured at JJMC and AHAB for 27 May to 20 August, 2004 are plotted in Figure 2. In Table 2, mean daily, mean maximum and mean minimum temperature, wind speed and relative humidity of these AWS is given. Daily mean temperature at AHAB and JJMC ranges between –8 and +12 °C (Fig. 2). The average air temperature at JJMC over the analyzed period is 5.3 °C, and exceeds the average air temperature at AHAB by only 1.2 °C (Table 2). The average temperature gradient between AHAB and JJMC is therefore 0.2 K per 100 m altitude, which is much smaller than the free air temperature gradient. We measured for 2004, a mean annual temperature of –11.0 °C for AHAB and –6.5 °C for JJMC (both HMP45AC Vaisala). This results in a steeper temperature gradient, of 0.6 K per 100 m altitude.

Daily mean air temperature and relative humidity at JJMC often reveal the same fluctuations as the measurements at AHAB (Fig. 2). However, when hourly mean air temperature and relative humidity (not shown) are considered, the relationship between AHAB and JJMC is not so strong. For hourly mean temperature, the correlation coefficient between AHAB and JJMC is 0.74 and the regression coefficient 1.13. For relative humidity, the correlation coefficient is 0.61 and the regression coefficient 0.79.

Two cold spells occurred during the summer of 2004: one between 6 and 10 July (JD 188-192), and another between 31 July and 2 August (JD 213-216). These cold spells coincide with periods of decreasing air pressure, increasing relative humidity, and also high wind speed (Fig. 2). During both periods, a low-pressure system was situated north of Alaska above the Arctic Ocean. This system caused a strong westerly flow at 500 hPa above the Eastern Brooks Range and high wind speeds at the surface. Both brought cold, humid air and snow from the northwest to the McCall Glacier area.

However, wind speed measured at JJMC did not peak during the second cold spell (especially 1 August: JD 214), while daily mean wind speed at AHAB shows a clear maximum. Since air temperatures at JJMC were below zero at that time, wind sensors were likely frozen. Or, the high wind speeds could have caused shaking of the weather station which loosened the connector or temporarily shorted something.

Mean, minimum and maximum wind speed at AHAB exceed those measured at JJMC (Table 2). When hourly averages are compared, wind speeds measured at AHAB and JJMC hardly show a relationship, with a standard deviation of 3.1 m s^{-1} and a correlation coefficient of 0.11. The explanation for this low correlation is that wind at JJMC is influenced by katabatic forcing and partly by the large scale wind, while wind at AHAB is mainly influenced by the large scale wind and perhaps also by local effects such as valley winds on warm days.

4.2 Daily variation and glacier wind

In Figure 3, mean daily variation in air temperature and wind speed is plotted for JJMC and AHAB. The air temperature at AHAB shows a clear daily fluctuation with a daily range of 5.3 °C. In contrast, JJMC hardly shows a daily cycle. This is explained by the fact that air temperature at JJMC is influenced by a surface temperature that is almost constantly at melting point. This cooling effect of the glacier is also nicely illustrated in Figure 4, where air temperatures of four stations are plotted for four clear-sky days. Air temperature at AHAB fluctuates with an amplitude of about 4 °C, and a daily temperature fluctuation is still visible for Station 1 in the accumulation area (Fig. 1). However, the daily cycle disappears at JJMC and is absent at Station 5. Figure 4 also demonstrates that the temperature gradient over the glacier is small. Mean temperature at the glacier snout (Station 5) over these four days exceeds the temperature at the glacier head (Station 1) by only 0.3 °C (0.04 K per 100 m). It is clear that in this situation, adiabatic heating of the air that travels down along the glacier is to a large extent compensated by cooling due to the exchange of sensible heat with the glacier surface (Greuell and Böhm, 1998).

Another marked result in the daily cycle of the meteorological variables is the absence of a wind speed maximum in the afternoon at JJMC (Fig. 3b). We notice that for JJMC, the mean daily variation in wind speed is small with a minimum in the afternoon, like at AHAB. Normally, wind speeds on valley glaciers increase in the afternoon (e.g. Van den Broeke, 1997; and Greuell and Smeets, 2001) as a consequence of an increased glacier wind due to a stronger temperature deficit in the afternoon (temperature difference between the near-surface layer and the ambient atmosphere). If the temperature at AHAB is regarded as a measure for the ambient atmosphere, the temperature deficit at McCall Glacier is largest at around 15 h (Fig. 3a). However, this is not translated into a wind speed maximum at JJMC (Fig. 3b). On the other hand, the air temperature at AHAB is possibly not a representative measure for the ambient temperature that overlies the glacier boundary layer and forces a glacier wind since the temperature at AHAB is influenced by warming and cooling of the rock-covered mountain slopes.

Oerlemans and Grisogono (2002) showed the relationship between wind speed and air temperature by plotting measured wind speed against air temperature measured on three glaciers: Morteratschgletscher in Switzerland, Vatnajökull in Iceland and the ablation zone of the West Greenland Ice Sheet. To investigate the glacier wind at JJMC in more detail, we did the same (Fig. 5). Figure 5a reveals a weak linear relationship between temperatures above melting point and wind speed at JJMC. It demonstrates that calm periods do not occur at temperatures above the freezing point and that increasing wind speeds are associated with increasing temperatures, indicative of katabatic forcing. Wind direction measured at JJMC also indicates that there is a persistent glacier wind (180º (south) is directly down-glacier) since it hardly varies below wind speeds of 5 m s^{-1} (Fig. 5b). Above this winds tend to come from the south-east, in the direction of a large hanging glacier. Explanations for the fact that glacier wind at McCall Glacier does not peak in the afternoon are given in section 6.1.

5. The energy balance and the specific mass balance

5.1. Methods

The energy balance of the glacier surface is described by the sum of the radiative components and the turbulent heat fluxes. The radiative components (incoming and reflected solar radiation, incoming and outgoing longwave radiation) are directly measured by the AWS. Since the radiation sensor was installed more or less parallel to the glacier surface, a correction for incoming solar radiation for tilt is not necessary. However, due to the poor cosine response of the CNR1 and the fact that the solar zenith angle exceeded 80° during about 25% of the measured period, we corrected incoming solar radiation using the method of ‘accumulated albedo’ (Van den Broeke and others, 2004). This method calculates incoming solar radiation from measured reflected solar radiation divided by the daily surface albedo derived from incoming and reflected solar radiation measurements.

Although we measured wind speed, air temperature and humidity at different levels, we calculated the turbulent heat fluxes using the bulk method (e.g. Munro, 1989). A profile method is not suitable here, since the difference between the wind speed at the two levels at JJMC (1.70 m and 3.05 m) is too small. The 3.05-m wind speed is on average only 0.01 m s^{-1} higher than the 1.70-m wind speed, and only during 32% of the measured period, wind speed at 3.05 m exceeds the wind speed at 1.70 m by the accuracy of the sensor (Table 1). This suggests a shallow katabatic flow with a wind speed maximum at only few meters above the surface. Under these conditions, a profile method cannot be used (Denby and Greuell, 2000).

As input for the bulk method, we used wind speed at 3.05 m and the finewire thermocouple temperature and the HMP45AC relative humidity at 2.06 m. The surface temperature was derived from measured outgoing longwave radiation and the Stefan-Boltzmann Law, assuming that snow and ice have unit emissivity in the longwave part of the spectrum. As is standard practice based on ice physics, we also assumed that the air just above the surface was saturated to calculate the surface vapor pressure from surface temperature. For this, we used air pressure measured at AHAB and an exponential decay with height to derive air pressure at JJMC.

Estimating the sensible and latent heat fluxes from Monin-Obukhov similarity theory also requires knowledge of the surface roughness length for wind speed, temperature and humidity. Wendler and Weller (1974) estimated a surface roughness length of 2.4 mm from wind profile measurements on McCall Glacier. We used this value and calculated the surface roughness length for temperature and humidity from the surface renewal model of Andreas (1987). The degree of turbulence also depends on the stability of the atmosphere: turbulent heat fluxes are suppressed in stable atmospheric conditions and enhanced in unstable conditions. On melting glaciers, stable conditions predominate because of positive air temperatures overlying the relatively cold ice. Stability functions account for this effect of stability on turbulence. We applied the stability correction functions from Holtslag and De Bruin (1988) for stable conditions because Andreas (2002) recommends these functions to use over snow and ice because of their good properties in very stable stratification. For unstable conditions, which only occurred 4% of the time, functions from Paulson (1970) were applied.

The sub-surface heat flux, which is small at JJMC, was calculated from the temperature gradient between the surface temperature and the ice temperature measured closest to the ice surface by the thermistor-string. Since the thermistor-string slowly melted out during the ablation period, the depths at which the thermistor-string measured changed. The depth of the thermistor closest to the surface used to calculate the sub-surface flux, and the exact depth was derived from the sonic height ranger data. The effective conductivity was calculated from Von Dusen's equation (Sturm and others, 1997), assuming a density of 300 kg m^{-3} for snow and 900 kg m^{-3} for glacier ice.

To calculate the specific mass balance, daily snowfall amounts were derived from changes in surface height measured by the sonic height ranger at JJMC. We used a snow density of 300 kg m^{-3} to translate snow depths into m w.e. Note that during the period that the sonic ranger was not operating (Fig. 8), we have no direct estimates of snowfall. For this period we estimated snowfall at JJMC using data from sonic height rangers located elsewhere on the glacier. We calculated the amount of melt from the surface energy balance and the amount of sublimation from the latent heat flux.

5.2 Energy fluxes

All energy fluxes presented in this study are defined as positive when directed towards the surface and therefore tending to warm or melt ice. Figure 6a depicts daily net solar radiation, net longwave radiation and the turbulent heat fluxes, calculated for the period from 27 May to 20 August, 2004. The largest flux over this period is outgoing longwave radiation (–313 W m^{-2}). It is nearly constant during the entire period since the surface was at melting temperature. The second largest energy flux is incoming longwave radiation (284 W m^{-2}). Incoming solar radiation shows the largest day-to-day fluctuations (from 32 to 284 W m^{-2}), and its average is 181 W m^{-2}. Average reflected solar radiation is –71 W m^{-2}, implying an average albedo of 0.39. The sensible and latent heat fluxes are 27 and 5 W m^{-2}, respectively. The sub-surface heat flux is –5 W m^{-2}. Net solar radiation is clearly the largest flux contributing to the surface energy balance. Except for a few days, net longwave radiation is negative.

The mean daily cycle in the energy fluxes is presented in Figure 7. Only solar radiation (incoming and reflected) reveals a strong daily fluctuation. Longwave radiation and the turbulent fluxes are nearly constant throughout the day, being a consequence of the small daily variation in air temperature and wind speed (Fig. 3).

Daily mean albedo is shown in Figure 6c. The measurements indicate that during both cold spells (section 4.1), the glacier surface was covered by fresh snow. During days that ice was exposed, the albedo was around 0.19, which is a measure for the ice albedo at JJMC. The measured minimum daily albedo is 0.17. This rather low value is discussed in section 6.2.

5.3 Sonic height ranger and ablation stake measurements

Estimating the specific mass balance from the sonic height ranger and the ablation stakes for comparison to the modeled specific mass balance is not a straightforward exercise in this case. Because the pole of the sonic height ranger melted out during the ablation period and was not reset for several weeks, the measurement record contains a data gap (Fig. 8). We therefore correlated the sonic height ranger data to the ablation stake data to reconstruct the measurement time-series. From the sonic height ranger we could derive the onset and termination of ice melt and from the ablation stakes the total amount of ice melt.

The distance between the sonic height ranger and the ice surface was 0.48 m when it was installed in spring 2004. All snow must thus have disappeared when the sonic ranger measured this distance (15 June). Next, we derived from the sonic height ranger that ice melt stopped around 23 August because the surface height remains constant after this date. The period of ice melt thus lasted more than two months. Ice melt between 15 June and 9 August was 1.79 m, according to the average of the two ablation stakes, and 0.39 m between 9 August and 23 August. Hence total ice melt between 15 June and 23 August was 2.18 m. The expected accuracy of this estimate is ± 0.1 m due to uncertainties in measuring the ablation stakes and spatial variation. A snow density of 300 kg m^{-3} and an ice density of 900 kg m^{-3} was used to translate the surface height changes measured by the sonic height ranger into m w.e.

5.4 Glacier melt, snow fall and the specific mass balance

Figure 6b shows daily melt rates calculated from the surface energy balance and snowfall as measured by the sonic ranger. The daily melt rate peaks in late June and early July, which is at the solar maximum, and declines throughout the summer.

Variations in the surface albedo (Fig. 6c) also impact the modeled melt rate: high albedo's coincide with low melt rates, as the high albedo caused by snowfall significantly decreases net solar radiation.

We calculated the specific mass balance over the period 15 June to 20 August (JD 167 to 233), since over this period the specific mass balance is known from the sonic height ranger and energy balance measurements are available. The sonic height ranger together with the ablation stake data measured a specific mass balance of –1.94 ± 0.09 m w.e. over this period (Fig. 8). The modeled specific mass balance calculated from the energy balance measurements is –2.06 m w.e. for this period (Fig. 8), which is an overestimation of 0.12 m w.e. or 6% compared to the sonic height ranger data. The modeled specific mass balance is the sum of 0.12 m w.e of snowfall, 0.003 m w.e. sublimation (i.e. deposition), and –2.18 m w.e of melt. The largest amount of discrepancy between the two time-series begins during the last major snowfall, when the sonic ranger tipped over. Therefore, we are likely underestimating the amount of snowfall.

In Figure 9, modeled daily specific mass balance is compared to specific mass balance derived from the sonic height ranger. The mean difference between the modeled and measured values is 1 mm w.e. and the standard deviation is 9 mm w.e. The latter value equals the accuracy of the sonic height ranger (Table 1).

Table 3 lists the mean surface energy fluxes over the period that the specific mass balance was calculated. The radiation balance contributes most to the energy available for melting (74%).

6. Discussion

6.1 Glacier wind and afternoon maximum

The results of section 4.2 demonstrate that at JJMC, the glacier wind does not peak in the afternoon, not even on clear-sky days with high solar radiation and high air temperatures. Afternoon wind speed maxima normally are found on glaciers at lower latitudes. Following the reasoning of Streten and others (1974), who carried out wind observations on McCall Glacier, there is probably insufficient contrast between the temperature of the ambient atmosphere and the glacier surface to produce a wind maximum during day since McCall is at a high elevation and latitude. During night, however, the temperature inversion reaches a maximum because of radiative cooling of the surface (Streten and others, 1974). This leads to a nocturnal wind speed maximum. This maximum is also indicated by our measurements (Fig. 3).

A further factor that explains the absence of the afternoon wind speed maximum at McCall is the up-glacier valley wind that likely retards the glacier wind during the afternoon (Streten and others, 1974). Such gentle winds that cause an up-glacier flow certainly occur now and then, since we regularly observed fog coming in during the afternoon from lower elevations. This fog typically creeps up the glacier to just above JJMC. The significance of this fog on spatial and temporal variations in mass balance has not yet been evaluated.

6.2 Sensitivity and accuracy of the calculations

To test the sensitivity in the calculated energy balance and the specific mass balance, we changed some input parameters and parameterizations. The resulting changes in the radiation balance, the turbulent heat fluxes and the specific mass balance over 15 June to 20 August, 2004 are listed in Table 4.

If the solar radiation sensor was inadvertently placed with a 4° tilt to the east relative to the surface, net radiation increases by 5 W m^{-2}. It is also shown in Table 4 that a correction for the stability of the atmosphere is very important. Applying no stability correction functions to calculate the turbulent fluxes for the analyzed period, in which stable conditions predominate, reduces the turbulent heat fluxes by 43%. The stability correction is large and has a strong impact on the calculated turbulent fluxes because the relatively low wind speeds at JJMC favor stable stratification,

The turbulent heat fluxes increase by 8 W m^{-2} when the 1.70-m wind speed is used as input for the calculations instead of the 3.05-m. Since wind speed at these two levels does not differ much (section 5.1), using wind speed from a lower level implies a change in the wind profile and an increase in the wind speed gradient, which leads to larger turbulent fluxes.

Table 4 also shows the importance of changes in the meteorological input variables air temperature, relative humidity, wind speed and net radiation. A positive change in the first three variables leads to an increase in the transport of sensible and latent heat towards the glacier surface, which causes an increase in ice melt at JJMC of about 0.1 to 0.2 m w.e. Increasing net radiation by 10 W m^{-2} causes a similar change in the melt rate at JJMC.

If ± 5 W m^{-2} and ± 9 W m^{-2} represent the accuracy of the radiation balance and the turbulent fluxes, respectively (Table 4), and we assume an accuracy of ± 3 W m^{-2} for the sub-surface heat flux, the standard error in the energy available for melting (125 W m^{-2}; Table 3) results in ± 11 W m^{-2}. This value (± 9%) represents the uncertainty in the calculated specific mass balance at JJMC over 15 June to 20 August 2004, which then becomes –2.06 ± 0.18 m w.e. The uncertainty is indicated by an error bar in Figure 8 and overlaps with the range within the measured specific mass balance is estimated.

6.3 Comparison to previous research and other glaciers

The mean air temperature at JJMC measured over the analyzed period (5.3 °C; Table 2) is larger than the mean temperature of the warmest month measured in 1971 (July), which was 3.2 °C (Wendler and Ishikawa, 1974). It is also larger than the mean 1970 July temperature, which was 3.8 °C (Wendler and Weller, 1974). 2004 was an exceptionally warm year in Alaska. For example, Barrow recorded the second warmest summer on record in about 100 years (G. Wendler, personal communication).

The measured minimum daily albedo in 2004 was 0.17 (section 5.2). This is smaller than a minimum albedo of 0.28 found by Wendler and Weller (1974) and 0.20 found by Wendler and Ishikawa (1974) for the same location in 1970 and 1971, respectively. Since 2004 was a year with numerous forest fires in Alaska, clearly observed increases in soot and dust concentrations on the glacier surface likely explain part of the difference.

The individual energy fluxes measured over the time that glacier ice was exposed are similar to those of Wendler and Weller (1974) and Wendler and Ishikawa (1974) (Table 3). They measured at the same location but for different summer periods. Still, the energy available for melting is higher in 2004 than in 1970 and 1971. This is due to the large positive sum of net radiation and the turbulent heat fluxes.

Due to high net radiation and the large sensible and latent heat fluxes caused by the exceptionally warm summer of 2004, 1.96 m w.e. of ice melt was measured at JJMC for the summer of 2004 (section 5.3). This is about double compared to the values reported by Wendler and others (1972), who measured about 1.20 and 0.78 m w.e. ice melt for 1969 and 1970, respectively, and larger than measured there since then.

Wendler and Weller (1974) and Wendler and Ishikawa (1974) already concluded that net radiation is the most important energy source for melting at McCall Glacier. Their measurements, collected in 1970 and 1971, showed that 87% and 60%, respectively, of the melting energy was supplied by net radiation during the period that glacier ice was exposed (Table 3). The present study indicates a value of 74% (section 5.4). These values compare well to similar measurements carried out in the ablation areas of other valley glaciers (Table 3): 65% for Morteratschgletscher in Switzerland (Klok and Oerlemans, 2002), 66% for Storglaciären in Sweden (Hock and Holmgren, 1996) and 76% for Pasterze in Austria (Greuell and Smeets, 2001). Nevertheless, net radiation and the turbulent heat fluxes are often smaller on McCall Glacier than on the glaciers at the lower latitudes due to lower temperatures and less incoming solar radiation. For instance, Table 3 shows that incoming shortwave and longwave radiation as well as the turbulent heat fluxes are higher on Morteratschgletscher and Pasterze than on McCall Glacier.

7. Conclusions

From the close correspondence between modeled and measured specific mass balance and our sensitivity analyses, it is clear that our instrumentation and methods are reliable enough to make robust conclusions regarding the surface energy balance. The warm summer of 2004 led to high melt rates on McCall Glacier, Alaska, and a specific mass balance at the glacier tongue of –1.94 ± 0.09 m w.e. between 15 June and 20 August, estimated from sonic height ranger and ablation stake data. The specific mass balance calculated from the surface energy balance for this period is –2.06 ± 0.18 m w.e., which agrees well with the measurements. The largest deviation between the modeled and measured specific mass balance begins when the sonic ranger failed and our model has poor input in regards to snowfall. Comparisons of modeled to measured daily specific mass balance have a mean difference of 1 mm. Our calculations showed that 74% of the melt energy is supplied by net radiation, which corresponds well both with prior measurements on McCall Glacier and with values found for glaciers at lower latitudes. Still, the turbulent heat fluxes and net radiation are often smaller at McCall Glacier than at lower-latitude glaciers due to colder temperatures and less incoming solar radiation.

Compared to energy balance and ablation measurements in 1970 and 1971 at the same location by Wendler and Weller (1974) and Wendler and Ishikawa (1974), summer ablation in 2004 was large. This melt is explained by the combination of a relatively low albedo, a high net radiation, and relatively large turbulent heat fluxes in 2004. 74% of the melt energy was supplied by net radiation in 2004, in between the two other years, but net radiation was about 45% higher than previous measurements. The low ice albedo in 2004 (0.19) is possibly due to the influence of soot and dust from forest fires that covered a large portion of the state. It is clear from these comparisons that there is a complicated interplay between the variables of the surface energy balance, and no single one can be isolated as having significantly changed between the time periods from this analysis, other than perhaps the temporarily-low albedo.

This study raises questions about the competition between valley and glacier winds. An analysis of meteorological data from the station at the glacier tongue and at a mountain ridge above the glacier reveal that the mean temperature gradient between the two sites is very small in summer (–0.2 K per 100 m altitude) because both stations measure in a different boundary layer. The air temperature at the mountain site shows a clear daily fluctuation due to local heating and cooling of nearby rock slopes. The station on the glacier tongue hardly shows a daily cycle because its temperature is influenced by the cooling effect of the glacier. Wind direction measurements and the fact that wind speed shows a weak linear relationship with air temperature lead us to believe that a glacier wind is often present at McCall Glacier. However, wind speed in the glacier's ablation area does not show a maximum in the afternoon, which is normally observed on glaciers at lower latitudes (Streten and others, 1974). This can be explained by a valley wind that retards the glacier wind during the afternoon or by McCall's high elevation and latitude, which lead to a small temperature contrast between the ambient atmosphere and the glacier surface (Streten and others, 1974).

These findings are of interest for modeling the spatial distribution of the energy and mass balance for McCall Glacier and need further investigation. Modeling the spatial distribution requires first of all knowledge about the spatial variation in air temperature and wind speed over the glacier. Often, it also requires information on the relationship between such air temperatures and wind speed and those outside the glacier boundary system when, for instance, meteorological reanalysis datasets are used as climate input. The results learned from this study will also inform future process studies that will facilitate a better understanding of the history of the glacier's dynamics and the changes in freshwater inputs to the Arctic Ocean in response to recent climate change.

Acknowledgments

We are grateful to Wouter Greuell and Gerd Wendler for commenting on the results. We would also like to thank Erin Pettit, Kristin Scott Nolan, and Bernhard Rabus for their help in establishing and maintaining the weather stations, Ken Irving for maintaining the telemetry system, and Larry Hinzman and the US Fish and Wildlife Service for support of the project. This work was funded by the National Science Foundation's Arctic System Science Program's Freshwater Initiative (Grant # 0229705); any opinions, findings, and conclusions or recommendations expressed in this material are those of the authors and do not necessarily reflect the views of the National Science Foundation.

References

Andreas, E. L. 1987. A theory for the scalar roughness and the scalar transfer coefficients over snow and sea ice. *Boundary-Layer Meteorol.*, **38**, 159–184.

Andreas, E. L. 2002. Parameterizing scalar transfer over snow and ice: a review. *J. Hydrometeorol.*, **3**(4), 417–432.

Denby, B. and W. Greuell. 2000. The use of bulk and profile methods for determining the surface heat fluxes in the presence of glacier winds. *J. Glaciol.*, **46**(154), 445–452.

Greuell, W. and R. Böhm. 1998. 2m temperatures along melting mid-latitude glaciers, and implications for the sensitivity of the mass balance to variations in temperature. *J. Glaciol.*, **44**(146), 9–20.

Greuell, W. and P. Smeets. 2001. Variations with elevation in the surface energy balance on the Pasterze (Austria). *J. Geophys. Res.,* **106**(D23), 31717–31727.

Hock, R. and B. Holmgren. 1996. Some aspects of energy balance and ablation of Storglaciären, northern Sweden. *Geografiska Annaler,* **78**A(2–3), 121–131.

Holtslag, A. A. M. and H. A. R. de Bruin. 1988. Applied modeling of nighttime surface energy balance over land. *J. Appl. Meteorol.*, **27**, 689–704.

Klok, E. J. and J. Oerlemans. 2002. Model study of the spatial distribution of the energy and mass balance of Morteratschgletscher, Switzerland. *J. Glaciol.*, **48**(163), 505–518.

Munro, D. S. 1989. Surface roughness and bulk transfer on a glacier: comparison with eddy correlation. *J. Glaciol.*, **35**(121), 343–348.

Nolan, M., A. Arendt, B. Rabus and L. Hinzman. In Press. Volume change of McCall Glacier, Arctic Alaska, from 1956 to 2003. *Ann. Glaciol.*, **42**.

Oerlemans, J. and B. Grisogono. 2002. Glacier winds and parameterisation of the related surface heat fluxes. *Tellus,* **54**A, 440–452.

Orvig, S. 1961. McCall Glacier, Alaska: Meteorological observations 1957-1958. *Arctic Institute of North America Research Paper,* No. 8, 30 pp.

Pattyn, F., M. Nolan, B. Rabud and S. Takahashi. In Press. Localized basal motion of a polythermal Arctic glacier: McCall Glacier, Alaska, U.S.A. *Ann. Glaciol.*, **40**.

Paulson, C. A. 1970. The mathematical representation of wind speed and temperature profiles in the unstable atmospheric surface layer. *J. Appl. Meteorol.*, **9**, 857–861.

Rabus, B. and K. E. Echelmeyer. 1998. The mass balance of McCall Glacier, Brooks Range, Alaska, USA: its regional relevance and implications for climate change in the Arctic. *J. Glaciol.*, **44**(147), 333-351.

Rabus, B. and K. E. Echelmeyer. 2002. Increase of 10 m ice temperature: climate warming or glacier thinning? *J. Glaciol.*, **48**(161), 279-286.

Streten, N. A., N. Ishikawa, and G. Wendler. 1974. Some observations of the local wind regime on an Alaskan Arctic Glacier. *Arch. Met. Geoph. Biokl.*, B(**22**), 337–350.

Sturm, M., J. Holmgren, M. König and K. Morris. 1997. The thermal conductivity of seasonal snow. *J. Glaciol.*, **43**(143), 26–41.

Trabant, D. C. and L. R. Mayo. 1985. Estimation and effects of internal accumulation on five glaciers in Alaska. *Ann. Glaciol.,* **6**, 113–117.

Van den Broeke, M. R. 1997. Structure and diurnal variation of the atmospheric boundary layer over a mid-latitude glacier in summer. *Boundary-Layer Meteorol.,* **83**, 183–205.

Van den Broeke, M. R., D. van As, C. H. Reijmer and R. S. W. van de Wal. 2004. Assessing and improving the quality of unattended radiation observations in Antarctica. *J. Atmosph. and Oceanic Technol*., **21**, 1417-1431.

Wakahama, G., D. Kuroiwa, T. Hasemi and C. S. Benson. 1976. Field observations and experimental and theoretical studies on the superimposed ice of McCall Glacier, Alaska. *J. Glaciol.,* **16**(74), 135–149.

Wendler, G., C. Fahl and S. Corbin. 1972. Mass balance studies on the McCall Glacier, Brooks Range, Alaska. *Arct. Alp. Res*., **4**(3), 211-222.

Wendler, G., N. Ishikawa and N. Streten. 1974.The climate of the McCall Glacier, Brooks Range, Alaska, in relation to its geographical setting. *Arct. Alp. Res.,* **6**(3): 307–318.

Wendler, G. and N. Ishikawa. 1974. The combined heat, ice and water balance of McCall Glacier, Alaska: a contribution to the International Hydrological Decade. *J. Glaciol*., **13**(68): 227–41.

Wendler, G. and G. Weller. 1974. A heat-balance study of McCall Glacier, Brooks Range, Alaska: a contribution to the International Hydrological Decade *J. Glaciol.,* **13**(67), 13–26.

Tables and figures

Table 1: Specifications of sensors measuring at JJMC, AHAB, Stations 1 and 5.

Sensor type	Parameter	Accuracy	Location
CNR1, Kipp & Zonen	shortwave & longwave radiation	± 10% for daily totals	JJMC
Met One 034B	wind speed wind direction	± 0.1 m s^{-1} or 1.1% ± 4°	JJMC, AHAB
HMP45AC Vaisala	air temperature relative humidity	± 0.2 °C (T = 20 °C) ± 0.4 °C (T = –20 °C) ± 2% (RH < 90%) ± 3% (RH > 100%)	JJMC, AHAB
Campbell SR50	surface height	± 0.01 m or 0.4%	JJMC
Vaisala CS105	air pressure	± 400 Pa	AHAB
Onset 12-bit Smart Sensor	air temperature	± 0.2 °C (T = 20 °C) ± 0.4 °C (T = –20 °C)	Station 1, Station 5

Table 2: Daily means, mean daily maximums and mean daily minimums for temperature, relative humidity and wind speed at JJMC and AHAB for the period 27 May to 20 August 2004.

	Air temperature (°C)	**Relative humidity (%)**	**Wind speed (m s^{-1})**
JJMC			
Mean	5.3	72	3.1
Maximum	8.2	88	5.9
Minimum	2.6	54	0.9
AHAB			
Mean	4.2	69	3.6
Maximum	8.1	85	7.1
Minimum	0.8	51	1.4

Table 3: Average daily energy fluxes in W m^{-2} *in the ablation area measured over the ablation period: incoming (S_{in}), reflected (S_{out}), net (S_{net}) solar radiation, incoming (L_{in}), outgoing (L_{out}), net (L_{net}) longwave radiation, net radiation (R_{net}), sensible (Q_H) and latent (Q_L) heat fluxes, sub-surface heat flux (G), and the energy involved in glacier melt (Q_M)). McCall 2004 are results of this study and McCall 1970 and 1971 from Wendler and Weller (1974) and Wendler and Ishikawa (1974), respectively. Data of the Pasterze in Austria are from Greuell and Smeets (2001) and of Morteratschgletscher from Klok and Oerlemans (2002).*

	McCall 2004	**McCall 1970**	**McCall 1971**	**Pasterze 1994**	**Morteratsch 1999/2000**
Period	15 June-20 August	18 July-28 August	17 June-22 July	22 June-6 August	all days with melting
S_{in}	166	169	230	256	255
S_{out}	–51	–79	–87	–53	–110
S_{net} (S_{in}+ S_{out})	115	90	143	203	145
α	0.30	0.48	0.38	0.21	0.43
L_{in}	290	?	?	299	310
L_{out}	–314	?	?	–315	–316
L_{net} (L_{in}+ L_{out})	–22	–24	–80	–16	–6
R_{net} (S_{net}+ L_{net})	93	66	63	187	139
Q_H	31	23	44	48	50
Q_L	6	–8	6	10	24
G	–5	–5	–8	–	–
Q_M	125	76	105	245	213

Table 4: Change in mean net radiation, the turbulent heat fluxes and the specific mass balance over 15 June to 20 August, 2004 with regard to the reference situation (where R_{net} is 93 W m^{-2}, Q_H+Q_L is 37 W m^{-2}, and the specific mass balance is –2.06 m w.e.) for varying parameters and parameterizations.

Change in parameter or parameterization	R_{net} **(W m^{-2})**	Q_H+Q_L **(W m^{-2})**	**Specific mass balance (m w.e.)**
Surface tilts 4° to the north [(1)]	+1	–	–
Surface tilts 4° to the south [(1)]	+4	–	–0.08
Surface tilts 4° to the east [(1)]	+5	–	–0.09
Surface tilts 4° to the west [(1)]	–3	–	+0.06
Surface roughness length * 10	–	+7	–0.13
Surface roughness length * 10^{-1}	–	–9	+0.13
No correction for stability [(2)]	–	+28	–0.45
3.05-m → 1.70-m wind speed [(3)]	–	+8	–0.14
2.06-m → 3.02-m air temperature and humidity [(4)]	–	+2	–0.04
Temperature + 1 K	–	+7	–0.11
Temperature – 1 K	–	–8	+0.11
Relative humidity + 10%	–	+8	–0.12
Relative humidity – 10%	–	–9	+0.12
Wind speed + 1 m s^{-1}	–	+14	–0.23
Wind speed – 1 m s^{-1}	–	–13	+0.19
Net radiation + 10 W m^{-2}	+10	–	–0.16
Net radiation – 10 W m^{-2}	–10	–	+0.15

(1) Tilt of the glacier surface with respect to the tilt of the solar radiation sensor.

(2) The stability correction functions to account for the stability of the atmosphere are not applied (Section 5.1).

(3) The 1.70-m wind speed is used as input for the calculation of the turbulent heat fluxes.

45) Air temperature and humidity at 3.02 m (HMP45AC Vaisala) are used as input for the calculation of the turbulent heat fluxes.

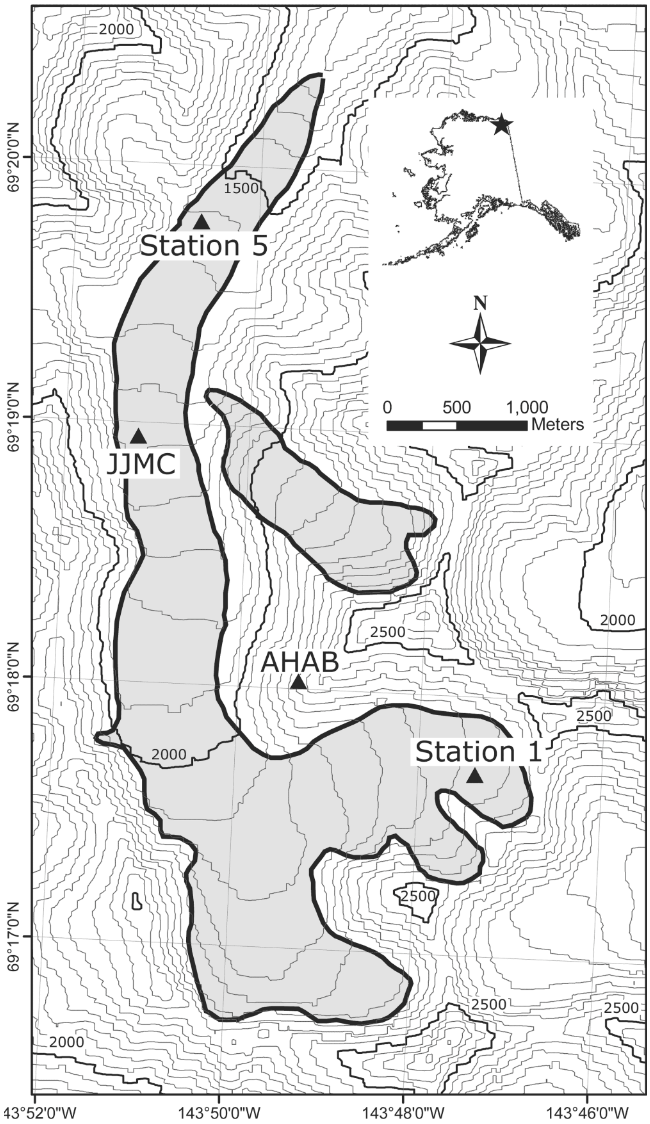

Figure 1: Location and map of McCall Glacier. The map indicates the locations of the automatic weather stations (AWS) JJMC and AHAB, and Stations 1 and 5. The contour map was created from a digital elevation model based on the 1956 USGS map (Demarcation Point B-5).

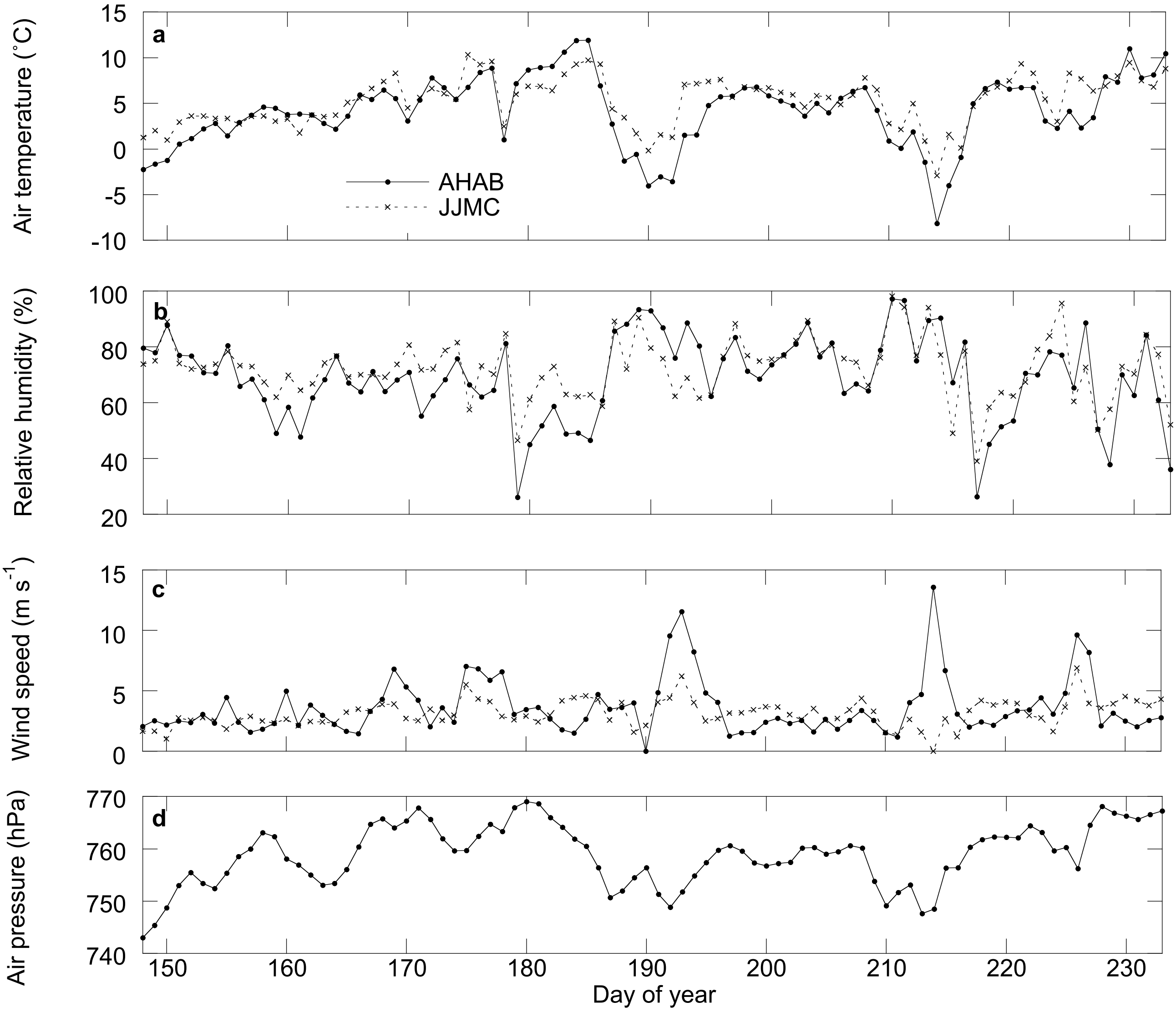

Figure 2: Daily mean air temperature (a), relative humidity (b), wind speed (c) and air pressure (d) at AHAB and JJMC for the period 27 May to 20 August 2004 (JD 148-233).

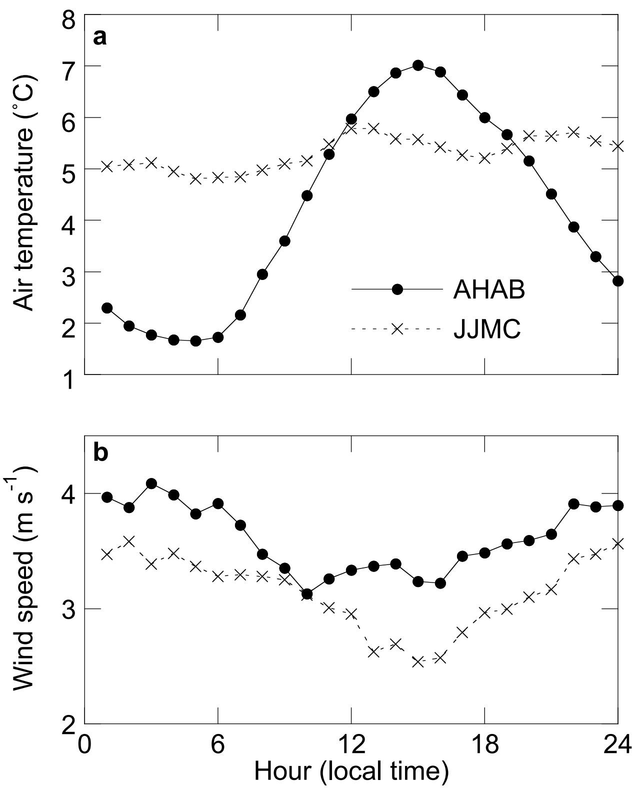

Figure 3: Mean daily fluctuation in air temperature (a) and wind speed (b) at AHAB and JJMC averaged over the period 27 May to 20 August 2004.

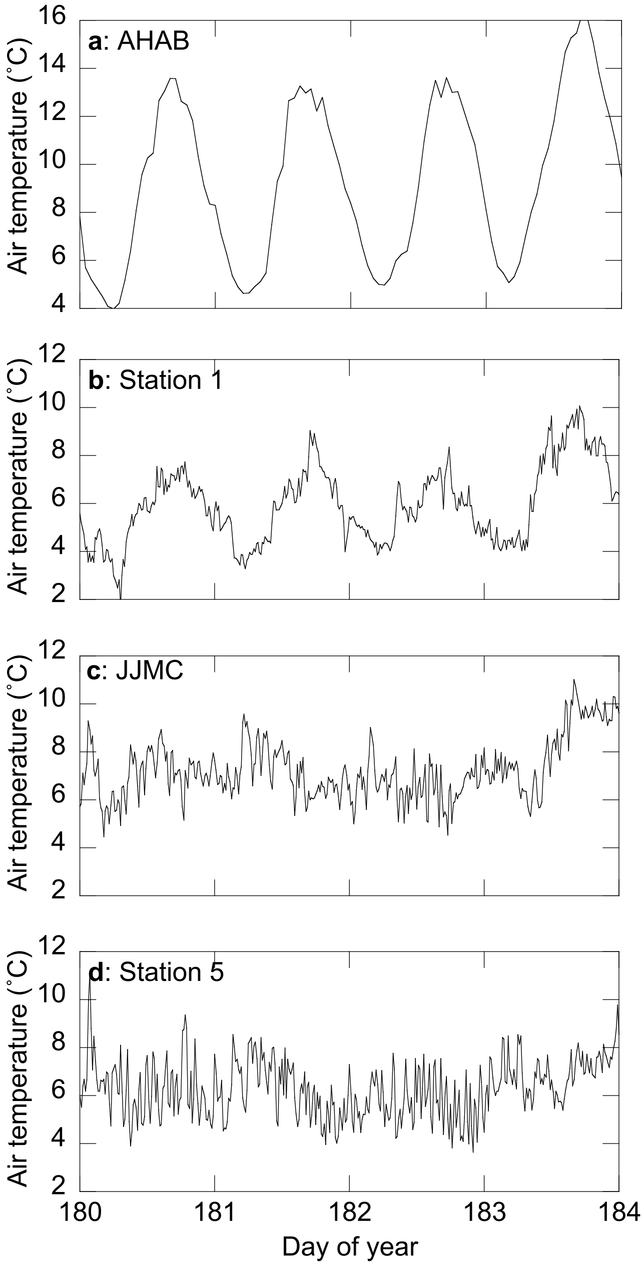

Figure 4: Air temperature for four clear-sky days at AHAB (a), Station 1 (b), JJMC (c) and Station 5 (d) shown in Figure 1. Measurements at AHAB are hourly averages, and at the other stations 15-minute averages.

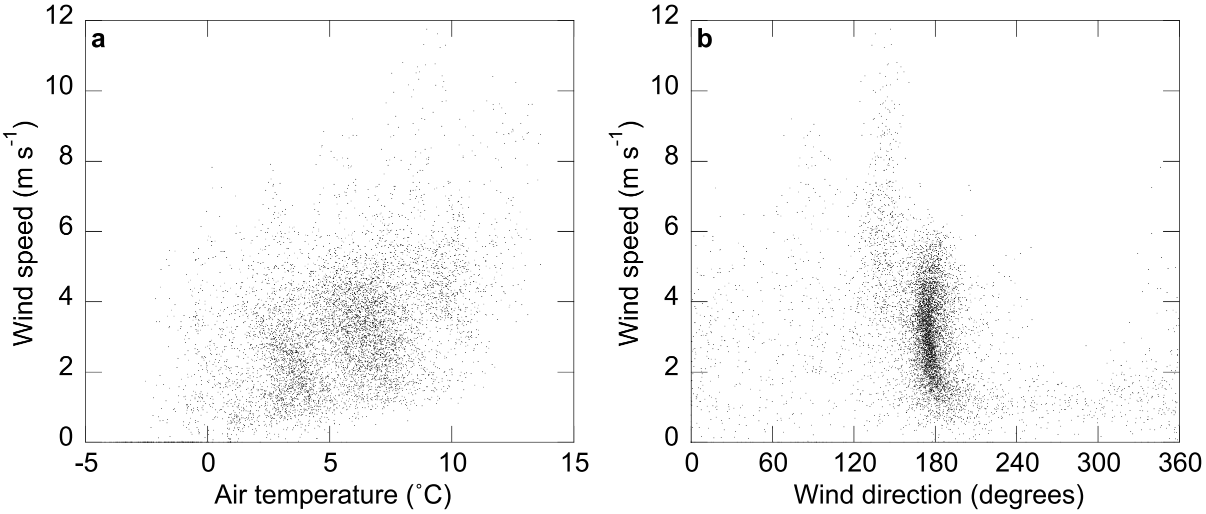

Figure 5: Wind speed at JJMC as function of air temperature (a), and wind direction (b) for the period 27 May to 20 August 2004 (15-minutes averages).

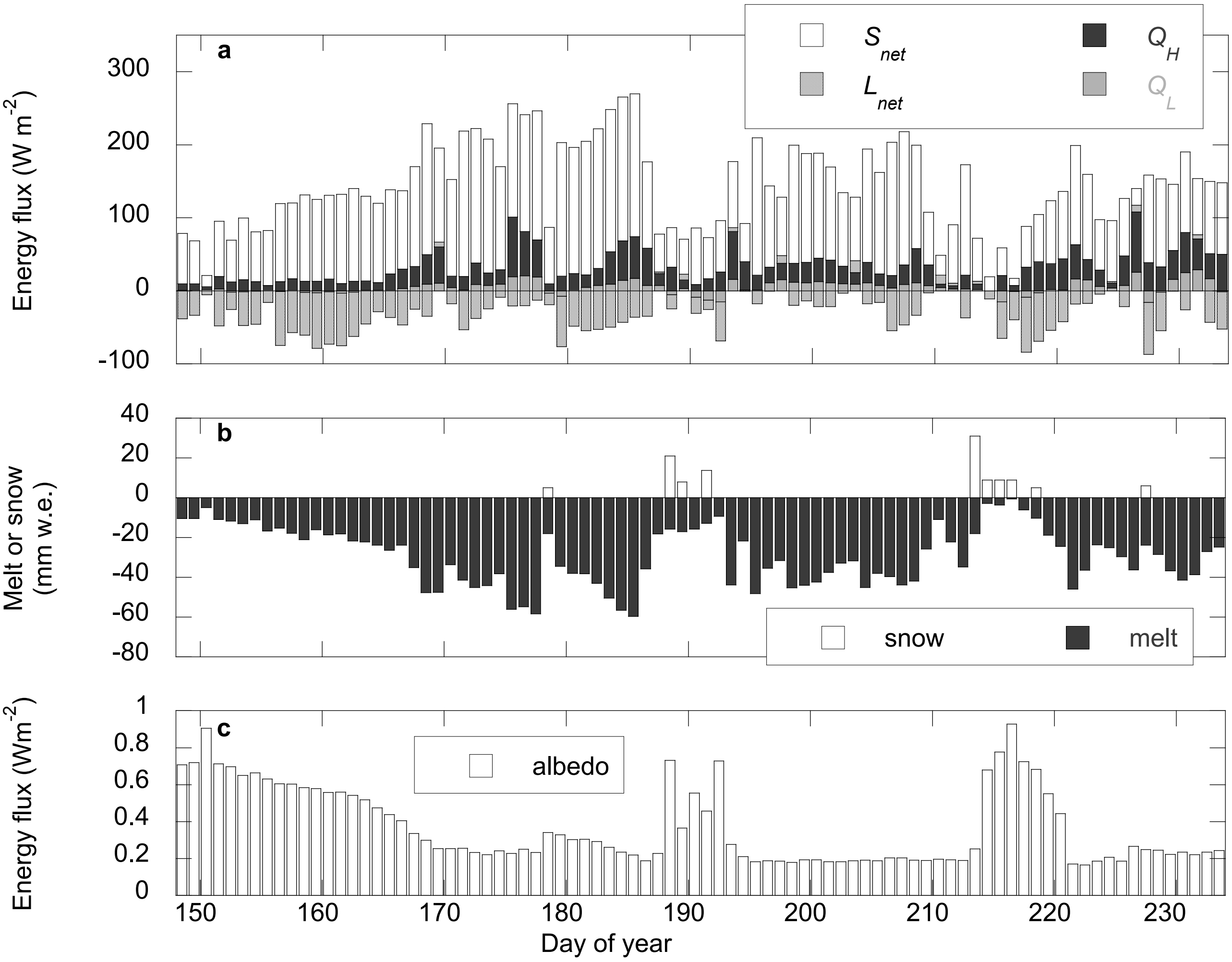

Figure 6: (a) Daily means of the net solar radiation (S_{net}), net longwave radiation (L_{net}) and the sensible (Q_H) and latent (Q_L) heat fluxes, (b) daily surface melt and snowfall and (c) daily mean albedo for the period 27 May to 20 August 2004 (JD 148-233).

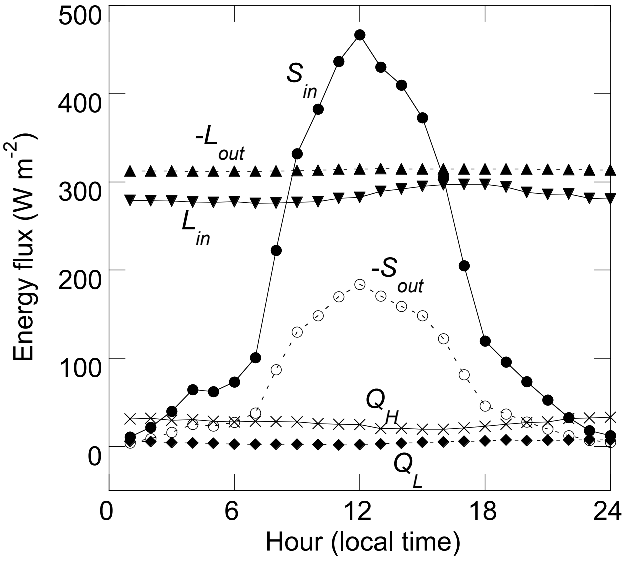

Figure 7: Mean daily cycle in incoming (S_{in}) and reflected (S_{out}) solar radiation, incoming (L_{in}) and outgoing (L_{out}) longwave radiation and the sensible (Q_H) and latent (Q_L) heat fluxes. The daily fluctuations are averages over the period 27 May to 20 August 2004.

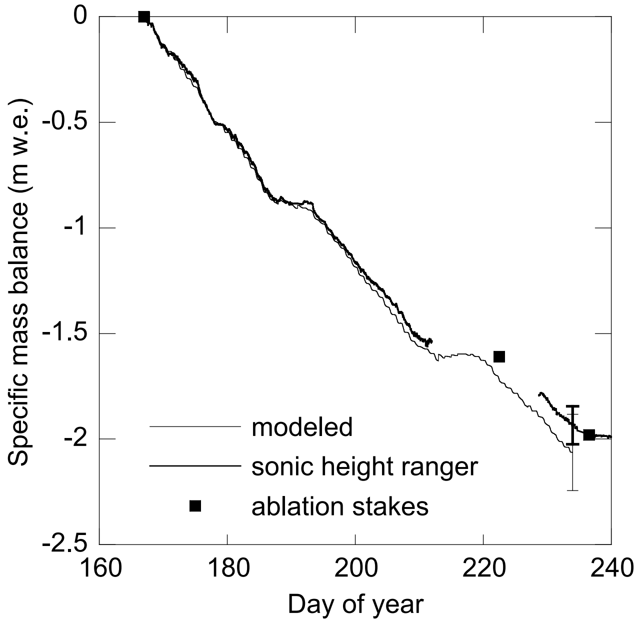

Figure 8: Specific mass balance as measured by the sonic height ranger and the ablation stakes (squares), and modeled from the surface energy balance. All records start at 15 June (JD 165) and the modeled specific mass balance ends at 20 August 2004 (JD 233). The error bars at 20 August indicates the accuracy of the modeled (thin error bar; section 6.2) and measured (thick error bar; section 5.3) specific mass balance.

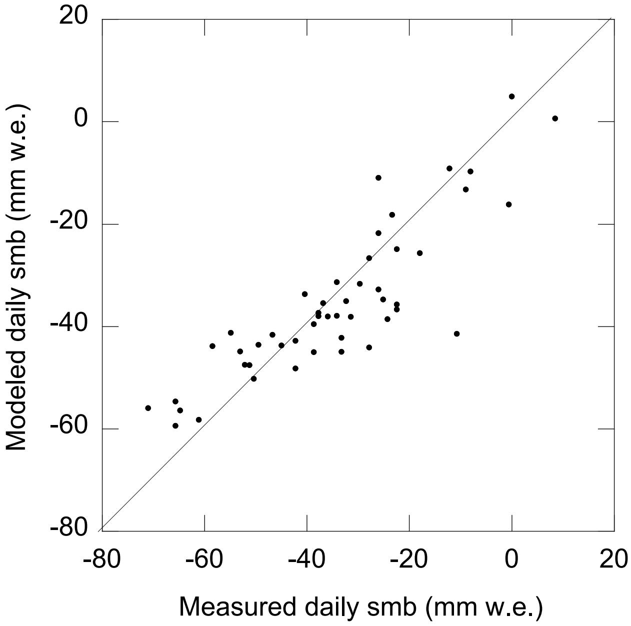

Figure 9: Modeled (derived from the surface energy balance) versus measured (derived from sonic height ranger and ablation stake data) daily specific mass balance (smb).